Engenharia Agrícola
ISSN: 1809-4430 (online)
www.engenhariaagricola.org.br | www.scielo.br/j/eagri

Scientific Paper
DOI: http://dx.doi.org/10.1590/1809-4430-Eng.Agric.v45e20250047/2025

DESIGN AND OPTIMISATION OF TEETH FOR THE 5TD-1200 SOYBEAN THRESHER

Yujiao Teng[1], Mengran Cui[1], Shunchang Guo[1], Bendi Qi[1], Xin Feng[1*]

[1*]Corresponding author. Engineering College, Northeast Agricultural University/Harbin, China.
E-mail: fx2020fx@163.com | ORCID ID: https://orcid.org/0009-0000-8790-0666

KEYWORDS

logarithmic spiral, arc-shaped threshing teeth, drum speed, proportion of broken grains, proportion of unthreshed grains.

ABSTRACT

Drum speed is a key parameter controlling threshing intensity: excessively high speeds cause a high proportion of broken grains (due to uneven impact), while excessively low speeds leave more unthreshed grains. It is difficult to balance these two effects by adjusting only the drum speed of a threshing device. Since threshing teeth structure affects the impact force on soybeans, optimising tooth shape is essential to address speed-related defects. This study presents a design for arc-shaped threshing teeth based on logarithmic spiral self-similarity, which maintains a relatively constant contact angle with the crop along the tooth surface. This makes the impact force smoother and more uniform (eliminating large fluctuations), simplifies the tooth profile, balances the impact force distribution, and effectively addresses the trade-off between the proportions of broken and unthreshed grains. Bench tests were conducted with drum speed as the influencing factor and the proportions of broken and unthreshed grains as evaluation indicators. Results showed that under optimal parameters, 15° arc-shaped teeth achieved a proportion of broken grains of 0.61% (0.68% lower than traditional teeth) and a proportion of unthreshed grains of 2.22% (only 0.1% higher). It is concluded that 15° arc-shaped teeth improve threshing device performance.

INTRODUCTION

Soybeans are an important crop in Asia, serving as a primary oilseed and major plant protein source with high economic value (Cabanos et al., 2021). Threshing, a critical stage in soybean harvesting, is mainly done by mechanical means; however, breakage from mechanical threshing may reduce seed germination and emergence rates, lowering the seed's economic value (Geremew et al., 2023). Threshing elements are key components of threshing devices, and their structure and parameters significantly affect the proportion of broken grains (Lian et al., 2022). Numerous studies show optimising structure and parameters can reduce the proportion of unthreshed and broken grains, thereby enhancing the economic benefits of a soybean crop.

To reduce the breakage of grains, experts have extensively studied the structures and action mechanisms of threshing elements. Chen et al. (2022) established a discrete element method to forecast impact-induced damage to maize kernels, revealing that impact force significantly influences maize quality. Dong et al. (2023) designed a rasp-bar threshing element with one bevelled end, mitigating impact forces. Liu et al. (2023) developed three rod tooth types (cylindrical, elbow, closed bow); simulations showed elbow rod teeth reduced drum-shaped cylinder threshing power consumption and improved performance. Su et al. (2018) designed an arc-surfaced nail tooth with increased contact area with maize ears; simulations indicated lower normal and tangential forces on ears vs. traditional trapezoidal nail teeth. Tan et al. (2023) designed a curved threshing tooth (10 equal-length short rod teeth), improving on the uneven striking force of traditional straight teeth. Zeng et al. (2022) designed direct-type, L-type, and logarithmic spiral guide vanes; simulations showed logarithmic spiral vanes enabled uniform airflow along the rotor cage circumference.

Scholars have also designed special tooth shapes (e.g., bevelled grain-poking teeth, elbow lever teeth) and optimised structures to reduce the proportion of broken grains. Since materials come into contact with teeth at all positions during threshing, the tooth design should focus

[1] Engineering College, Northeast Agricultural University/Harbin, China.

Area Editor: Fábio Lúcio Santos
Received in: 3-29-2025
Accepted in: 9-18-2025

on innovation in terms of the overall structure to reduce the unevenness in impact force. Based on the constant-angle characteristic of logarithmic spirals, this study proposes an arc-shaped design for threshing teeth, which can enable a relatively constant contact angle to be maintained with the crop along the tooth surface, making the impact force smoother and more uniform and avoiding large fluctuations. Since the different structural parameters of arc-shaped threshing teeth affect threshing performance differently, further systematic research on the key parameters is needed.

Threshing quality is significantly affected by the operating parameters of threshing devices. Experts have studied how various parameters influence threshing indicators: Srison et al. (2016) showed rotor speed significantly affects the proportion of broken maize grains, which increases as rotor speed rises. Yang et al. (2024) found that besides moisture content, drum speed has the greatest impact on the threshing performance of axial bow-tooth sunflower threshing devices. Jin et al. (2021) investigated how forward speed, drum speed, threshing gap, and deflector angle affect the proportions of broken and unthreshed grains under different threshing drum structures; field and orthogonal tests revealed these two proportions are significantly affected by drum speed. Numerous studies confirm that drum speed strongly affects a threshing device’s performance and operation quality indicators. Thus, the structural design and testing of new threshing elements should be carried out at appropriate drum speeds.

In summary, severe grain breakage during threshing causes grain loss, with a direct impact on food security. It is difficult to strike a balance between the proportions of broken and unthreshed grains based solely on adjustments to the drum speed, meaning that novel shapes for the threshing teeth are essential to improve device performance. Unlike existing fixed-curvature, arc-shaped threshing teeth, the ones developed in this study are based on logarithmic spirals, and enable a relatively constant contact angle to be maintained with the crop along the tooth surface, making the impact force smooth, uniform and free from large fluctuations. Single-factor tests are carried out to explore the influence of drum speed and this tooth shape on threshing performance. Under optimal conditions, the proportions of broken grains and unthreshed grains are lower than for traditional straight teeth, thus demonstrating the applicability and feasibility of this design.

MATERIAL AND METHODS

Soybean material

The soybean variety "Heihe 43", which is widely planted in Northeast China, was selected as the basis for the bench tests in this study. The relevant parameters for soybeans were determined according to the Chinese National Standard GB/T 5262-2008, entitled "General Rules for the Determination of Test Conditions for Agricultural Machinery" (Hao et al., 2008). All parameters were expressed as average values (Table 1).

TABLE 1. Basic parameters for soybeans.

Property	Value
Stem height	84.36 cm
Number of pods per plant	56
Number of seeds per plant	153
Number of seeds per pod	2.57
Hundred-grain weight	21.33 g
Grain mass per plant	32.63 g
Stem diameter	6.55 mm
Grain moisture content	16.4%

Threshing elements

Arc-shaped threshing element

Arc-shaped teeth can give an increased contact area with the material (Su et al., 2018) and can change the angle of impact between the threshing element and the grain. This reduces the impact force at the end of the threshing teeth, away from the threshing drum, thereby ensuring a more uniform distribution of impact force within the threshing space (Tan et al., 2023). A logarithmic spiral exhibits self-similarity and superior uniformity (Jia et al., 2025). In this study, arc-shaped threshing teeth were designed based on the logarithmic spiral. The primary parameters of these arc-shaped threshing teeth are their geometric dimensions, which include the vertical distance from the endpoints of the arc-shaped teeth to the threshing drum, the cross-sectional diameter of the arc-shaped teeth, and the bending angles, defined as the included angles between the tangents at the two endpoints of the arc-shaped teeth.

Reports in the existing literature indicate that the concave plate clearance of a soybean threshing drum is generally adjusted within the range 20–40 mm (Jin et al., 2021; Gao et al., 2015). In this case, the distance between the lowest points of the threshing elements and the concave plate of the small-scale soybean thresher used for the bench test was set to 70 mm. To avoid interference between the arc-shaped threshing teeth and the frame during the test, while ensuring the principle of single variable, the vertical distances from the endpoint of the arc-shaped teeth to the threshing drum were set to the same length as traditional threshing teeth, measuring 48 mm, resulting in a concave plate clearance of 22 mm. The flexible threshing teeth are bent into a certain arc shape during threshing. More favourable threshing characteristics could be obtained using threshing teeth with diameters of 4, 6 and 8 mm, and in particular, teeth with a diameter of 6 mm give relatively low proportions of broken and unthreshed grains (Xie et al., 2009). Since the diameter of traditional threshing teeth was measured as 6 mm, the cross-sectional diameter of the proposed arc-shaped teeth was also taken as 6 mm.

The bending angles of the arc-shaped teeth should be within a certain range, neither too large nor too small. If the bending angles are too small, the vertical impact forces on the arc-shaped teeth are large, and the outer-layer materials are subjected to high vertical impact forces. This leads to an uneven distribution of impact forces within the threshing space, making it difficult to complete the threshing operation. In general, the bending angles should not be less than 10°. In addition, if the bending angles are too large, the grasping abilities of the nail teeth will be weakened, the residence times of the materials in the threshing drum will be increased, and the threshing space will be blocked; hence, the bending angles should not exceed 30° (Tan et al., 2023; Liu et al., 2017). In our experiment, it was found that when the threshing tooth angle was 30°, the proportion of broken grains was very low, but the proportion of unthreshed grains failed to meet the national standard requirements for all ranges of drum speed. We selected six levels for the experiment; however, the results showed that indicators for two levels failed to meet the national standard requirements for all drum speeds. We therefore chose the remaining four levels, after excluding the substandard ones. The initial range for the bending angle of the arc-shaped teeth was set between 10° and 25°. Preliminary tests have shown that bending angles of 10°, 15°, 20°and 25° cover the critical points at which the threshing performance changes significantly; hence, these angles were selected for detailed analysis.

The shape of the logarithmic spiral curve was determined using [eq. (1)]. To make the logarithmic spiral expand in a limited space and to create a suitable shape, the value of a was taken as 0.1, while the value of b was taken as −0.1 to create a logarithmic spiral with a relatively gentle clockwise rotation. In this way, a logarithmic spiral with typical contraction characteristics and moderate rotational speed was obtained, which facilitates the mathematical calculations and parameter determination. The logarithmic spiral shape was determined using MATLAB, as shown in Figure 1. By combining [eq. (1)] and the logarithmic spiral shape, the parameters and line types corresponding to the six bending angles were determined using MATLAB. For values of a = 0.1 and b = −0.1, a bending angle of 10° could be obtained by extracting the range of the variable θ from 2π to 2.0556π; an angle of 15° was obtained for values from 2π to 2.0835π; an angle of 20° was obtained for values from 2π to 2.1115π; and an angle of 25° was obtained with values from 2π to 2.1389π. The line types corresponding to each bending angle are shown in Figure 1.

After we had established a 3D model based on the selected line types, 3D printing technology was adopted for precise manufacturing. Due to considerations of both cost and threshing strength, stainless steel was selected as the material for physical processing. Finally, the optimal bending angle was determined through bench tests.

$$r = a \cdot e^{b \cdot \theta} \tag{1}$$

where r is the polar radius, defined as the distance from the pole to a specific point on the curve, and θ is the polar angle, representing the angle between the polar axis and the line segment connecting the pole and the point on the curve. a and b are constants.

To clarify the basis for selecting the bending angles of the arc-shaped threshing teeth and more clearly assess the law governing the change in threshing performance as the bending angle changes, we conducted a theoretical analysis of the arc-shaped threshing teeth.

The force exerted by the threshing teeth on soybeans is a core factor affecting threshing performance, with the most significant impact arising from the highest point of the arc-shaped threshing teeth on the material. In this analysis, we consider the soybeans at the highest point (denoted as O′) as the research object, and decompose the resultant external force acting on the centroid of a soybean from the threshing teeth. The force composition is shown in Figure 2.

The definitions of each parameter are as follows: F_1 is the resultant external force exerted by the teeth on the soybeans; F is the striking force of the teeth on the soybeans; O is the axis of the threshing drum; O′ is the highest point of the teeth; F_n is the component of the force F in the direction perpendicular to the tangent at O′; F_t is the component of F in the direction of the tangent at O′; F_f is the friction force between the soybeans and the teeth; α is the angle between F and F_n; μ is the friction coefficient between the soybeans and the teeth; Δv is the linear velocity of the drum at O′; m is the mass of the soybeans; Δt is the impact time between the soybeans and teeth; ω is the angular velocity of the drum; and L is the length of the line between O and the centroid of the soybean .

Based on the above parameters and the theorem of momentum, the relationships of the resultant external forces on the soybeans can be derived as shown in [eq. (2)]:

$$\begin{cases} F_1 = F + F_f \\ F_n = F \cdot \cos\alpha \\ F_t = F \cdot \sin\alpha \\ F_2 = F_n \\ F_3 = F_t - F_f \\ F_f = \mu \cdot F_2 \\ F_1 = \dfrac{m \cdot \Delta v}{\Delta t} \\ \Delta v = \omega \cdot \mathrm{L} \end{cases} \tag{2}$$

where F_2 is the resultant force exerted on the soybeans along the direction perpendicular to the tangent at O′; and F_3 is the resultant force exerted on the soybeans along the tangent direction at O′. To ensure the validity of the comparison between arc-shaped threshing teeth with different bending angles, key variables were controlled at the design stage: the length L of all the teeth was kept consistent, and the drum speed was the same. If it is also assumed that the impact time Δt and mass of soybeans m are the same, the resultant force F_1 exerted by arc-shaped threshing teeth with different bending angles on soybeans is consistent. In addition, since the friction force F_f is much smaller than the striking force F, its impact on the resultant force can be neglected, and we assume $F_1 \approx F$ in this analysis. Since the material of the arc-shaped threshing teeth in the experiment is uniform and the variety of soybeans is fixed, the friction coefficient μ is also a constant.

To quantify the effect of the bending angles on the force, calculations for α were conducted using MATLAB, in which the logarithmic spiral formula and the θ ranges were combined as described earlier. The results show that when the bending angle of the teeth increases from 10° to 25°, α are 3.2°, 5.7°, 7.8°, and 9.5° in sequence, and the increase range of α gradually decreases as the bending angle increases.

From [eq. (2)], we can derive [eq. (3)]:

$$\begin{cases} F_2 = \dfrac{m \cdot \omega \cdot \mathrm{L}}{\Delta t} \times \cos\alpha \\ F_3 = \dfrac{m \cdot \omega \cdot \mathrm{L}}{\Delta t} \times \left(\sin\alpha - \mu \cdot \cos\alpha\right) \end{cases} \tag{3}$$

From [eq. (3)], it can be seen that when the bending angle is increased from 10° to 15°, the increase in the range of α is the largest, and F_2 decreases significantly, which can reduce the striking force on the soybeans. The value of $\tan\alpha$ is relatively small at this stage, meaning that friction can effectively prevent the soybeans from slipping. Under the combined effect of these two factors, the proportion of broken grains decreases significantly. When the bending angle is increased further from 15° to 25°, the increase range of α becomes smaller, and the decreasing amplitude of F_2 slows down accordingly, leading to a gradual weakening of the downward trend in the proportion of broken grains. At the same time, $\tan\alpha$ continues to increase, resulting in a larger F_3. This weakens the gripping force of the teeth on the material, further increasing the number of collisions between the material and the teeth, and eventually causing the proportion of broken grains to shift from decreasing to increasing.

In summary, the proportion of broken grains is lowest when the bending angle of the arc-shaped threshing teeth is 15°, and it shows an overall trend in which it first decreases and then increases. The proportion of unthreshed grains shows an opposite trend to the proportion of broken grains. This finding provides critical theoretical support for selecting the bending angle of new arc-shaped threshing teeth.

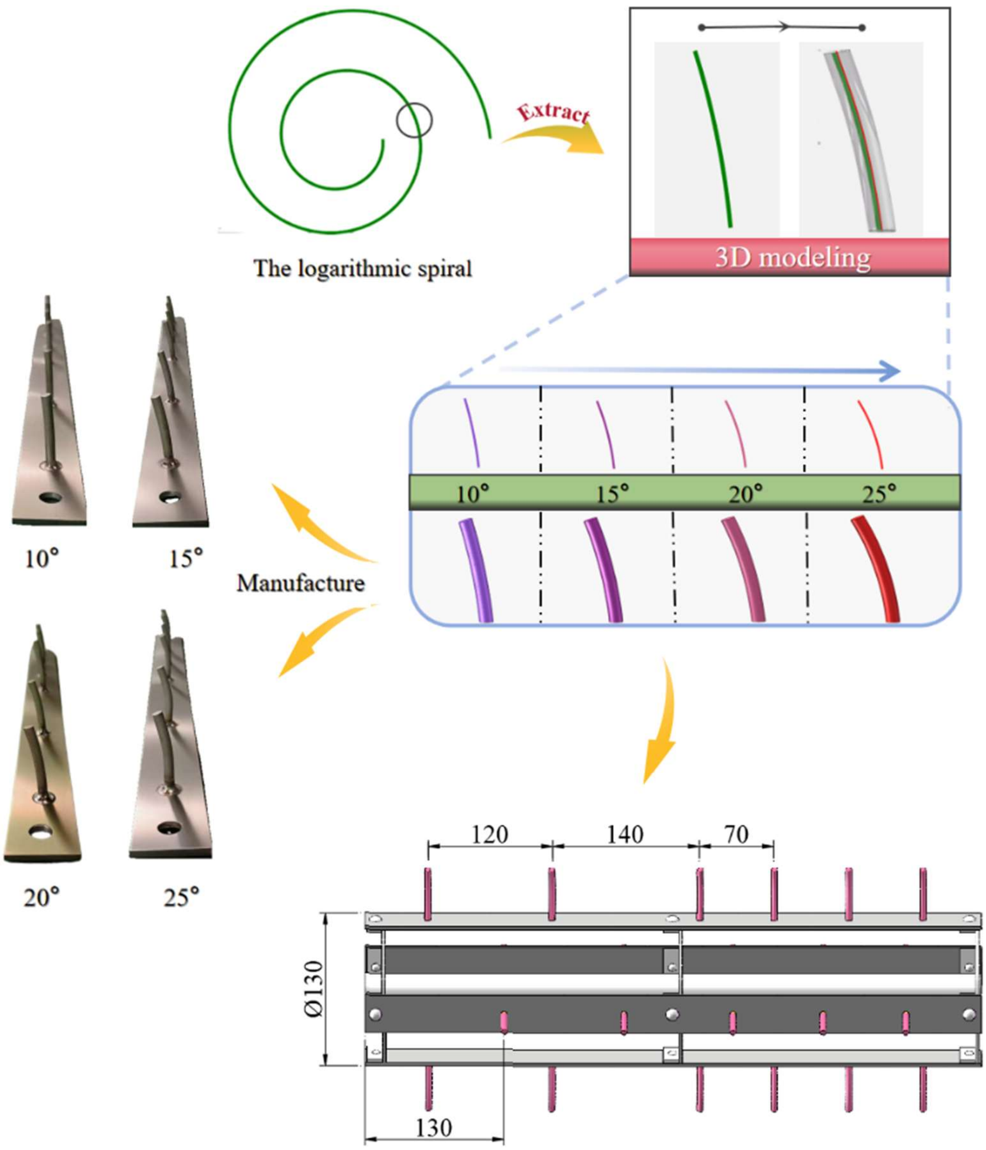

FIGURE 1. Structure of the proposed arc-shaped teeth.

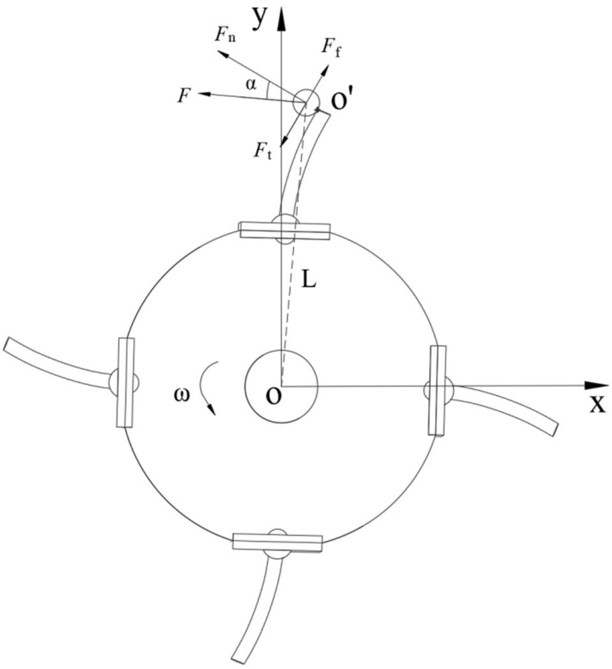

FIGURE 2. Decomposition of forces from the arc-shaped threshing teeth on the soybeans.

Threshing bench

The threshing bench used for testing mainly consists of a frame, a frequency converter, a transmission system, a threshing device, and a cleaning device, as shown in Figure 3. The frame is equipped with a feeding port, an outlet, and a discharge port, while the transmission system is composed of a drive motor, pulleys, and a transmission belt. The threshing device consists of a threshing drum and a concave plate. The threshing drum includes a spindle, fixing plates, and threshing teeth, which include traditional threshing teeth and four types of arc-shaped teeth. The traditional threshing teeth are rod-shaped teeth that are bent at an angle of 13.5°; after this bend, both ends of each tooth remain straight. The lower part of each traditional threshing tooth is installed at an 8° angle to the cross-sectional diameter of the threshing drum at the centre of the tooth at the bottom. The cleaning device includes a sieve plate and a fan.

Although the cleaning device is not the core component studied in this paper, it is indispensable for the test, for two reasons. Firstly, it ensures alignment with the actual operating scenarios. The test bench takes the 5TD-1200 soybean thresher as the prototype, and the cleaning device is a standard component of an actual thresher (enabling integration between threshing and cleaning). The presence of this device ensures that the test system is consistent with actual application scenarios, thereby preventing discrepancies between test conditions and real-world operating scenarios due to simplification of the device. Secondly, it can improve the measurement efficiency and accuracy. Direct weighing of materials after threshing makes it difficult to identify and separate target grains due to interference from impurities. The cleaning device can quickly remove large impurities while retaining beans and unthreshed pods through the use of a sieve plate matching the size of the soybeans, which reduces the workload and errors due to manual sorting and thus improves measurement efficiency. Notably, the presence of the cleaning device does not affect the measurement accuracy of the threshing parameters. Calculation of the core evaluation indicators considered in this study (the proportions of broken and unthreshed grains) is based on the state of the bean–pod (including grains) mixture after threshing. The cleaning device is only used to separate impurities such as straw and broken leaves from the mixture, in order to quickly collect pure grains for quality weighing. Furthermore, the interaction between the sieve surface and materials during the cleaning process does not cause threshing or grain breakage, and thus has no effect on the calculation of the threshing indicators. The parameters of the cleaning device used in the test, such as the fan speed and inclination angle of the sieve plate, were calibrated in accordance with GB/T 5982-2017 and kept fixed; this component only achieves physical separation, and does not change the broken state of the beans after threshing.

During operation, soybean stalks are fed into the machine through the feeding port and threshed between the threshing drum and the concave plate. After threshing, beans and mixed debris pass through the concave plate and fall onto the sieve plate for cleaning with the aid of the fan. The straw debris is discharged through the outlet, which is equipped with a mesh structure to separate beans mixed with straw. The screened materials slide down onto the sieve plate through an iron plate set below, and are then cleaned using the fan. The cleaned beans are then discharged through the discharge port into a metal frame below. The threshing process is shown in Figure 3.

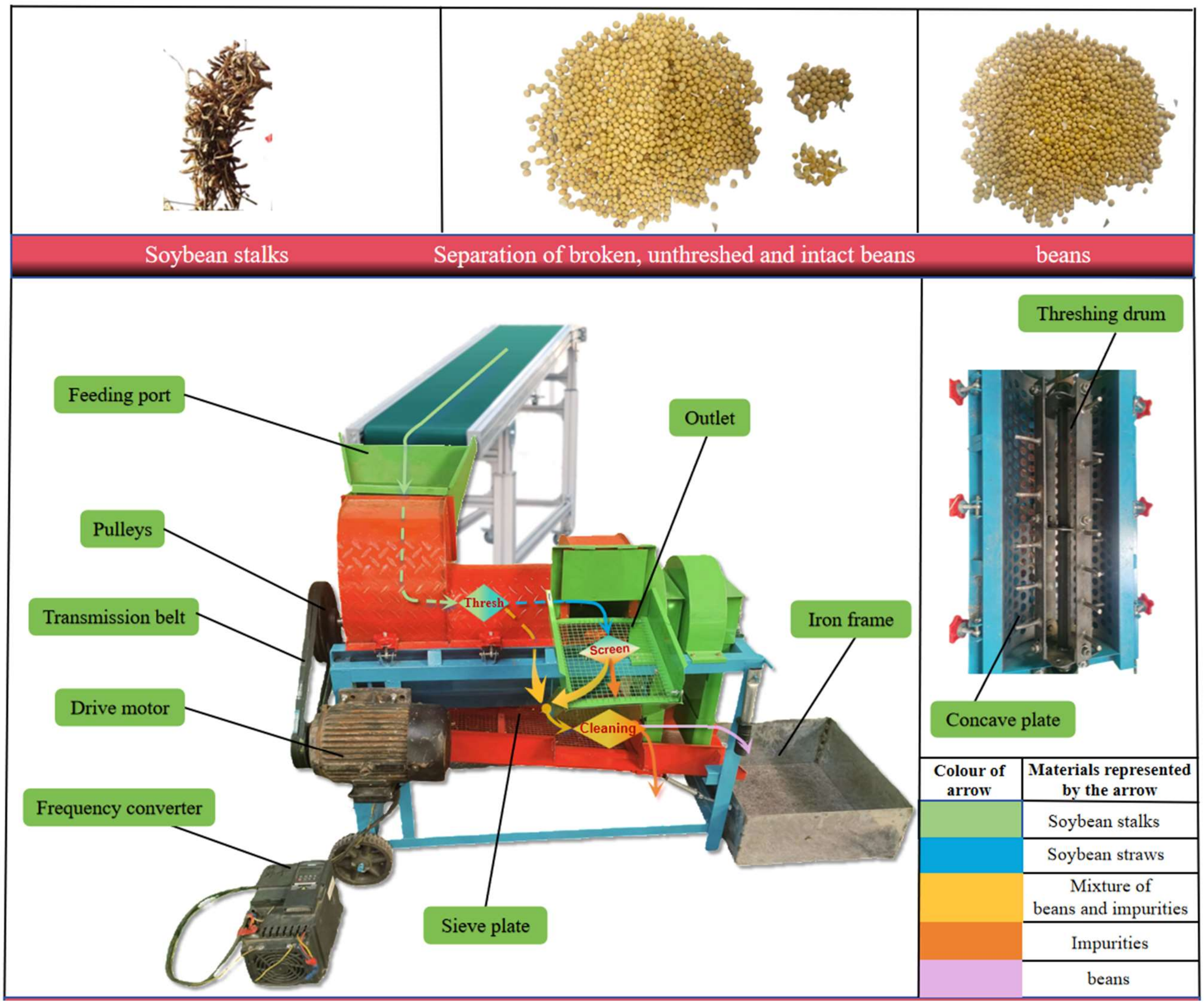

FIGURE 3. Threshing device.

Test method

Soybean threshing tests were carried out in accordance with the Chinese national standard GB/T 5982-2017, entitled "Test Methods for Threshers" (Deng et al., 2018). Taking the drum speed (X_1) as the influencing factor, and the proportions of broken grains (Y_1) and unthreshed grains (Y_2) as the evaluation indicators, a single-factor experiment was designed. Based on the field pre-test and the "Agricultural Machinery Design Handbook (Volume II)", the drum speed was set to 400, 450, 500, 550, and 600 r·min^{-1}. In addition to the drum speed, the feeding rate, another key parameter affecting threshing performance, was also examined through a literature review and pre-tests. Prior to the formal experiment, three feeding rates (0.3, 0.5, and 0.7 kg·s^{-1}) were used for pre-tests. The results showed that at 0.3 kg·s^{-1}, the efficiency was low and the deviation of single test data was relatively large; at 0.7 kg·s^{-1}, accumulation of material was obvious, and the proportion of unthreshed grains increased significantly, whereas at 0.5 kg·s^{-1}, the material flow was stable, and the proportions of broken and unthreshed grains were within a reasonable range, which could accurately 'reflect the threshing performance differences between different tooth shapes. Furthermore, this feeding rate met the production requirements for soybean threshing (Gao et al., 2015), and was therefore determined as the test parameter. Pre-test results showed that when the feeding amount per test exceeded 2.5 kg, material accumulation occurred in the conveying device, leading to unstable threshing and large deviations in the obtained data. The total feeding amount of 2.5 kg per test served three key purposes. Firstly, it enabled us to collect a sufficient quantity of post-threshing materials (e.g. grains, unthreshed pods). Secondly, these materials met the required sample size for calculating the proportions of broken and unthreshed grains, which effectively reduced the rate of random errors. Thirdly, it represented a balance between test efficiency and data validity. In view of this, the threshing duration for a single test was set to 5 s, which gave a feeding amount of 2.5 kg per test.

Bench tests were conducted separately for traditional threshing teeth and four types of arc-shaped threshing teeth with different bending angles. Before the formal tests, the drum speed was calibrated using a tachometer to ensure that the frequency of the variable frequency drive (VFD) corresponded to the drum speed, and the drum speed was adjusted based on the VFD. During each experiment, the mass of the required materials was measured using an electronic scale. The VFD was adjusted to obtain the required drum speed. Once the drum speed had stabilised, the material was evenly spread on the conveyor belt to ensure a feeding rate of 0.5 kg·s^{-1} (Gao et al., 2015). After the test, all the threshed soybeans were collected, and the proportions of broken and unthreshed grains were calculated. Each test was repeated three times, and the average values for the proportion of broken and unthreshed grains were taken. Finally, the performance curves were plotted based on the obtained data, as shown in Figures 4 and 5. The formulae used to calculate the proportions of broken grains (Y_1) and unthreshed grains (Y_2) were as follows:

$$Y_1 = \frac{m_p}{m_1 + m_p + m_w} \times 100\% \tag{4}$$

$$Y_2 = \frac{m_w}{m_1 + m_p + m_w} \times 100\% \tag{5}$$

where m_p is the mass of the broken grains, g; m_w is the mass of the grains inside soybean pods, g; and m_1 is the mass of the intact grains (excluding the grains inside the pods), g.

RESULTS AND DISCUSSION

Influence of drum speed on the proportion of broken grains for different tooth shapes

Figure 4 shows the variation in the proportion of broken grains with an increase in drum speed under different tooth shapes. As the drum speed increases, the proportion of broken grains initially decreases and then increases, since at lower drum speeds, the threshing intensity is lower, and the separation time is longer. As a result, the number of collisions between the grains and the threshing teeth is increased, and the friction of the materials is likely to be increased due to the accumulation of the materials.

The proportion of broken grains is high for two reasons. As the drum speed increases, the impact force on the grains from the threshing teeth is increased, which causes the grains to be rapidly threshed and sent out of the threshing drum before being broken. This reduces material accumulation and consequently lowers the proportion of broken grains (Fang et al., 2024). However, as the drum speed continues to increase, the impact force on the grains becomes excessive, causing the proportion of broken grains to increase (Xing et al., 2024). As the bending angle of the arc-shaped teeth increases, the proportion of broken grains first decreases and then slowly increases, and the lowest proportion of broken grains occurs at a bending angle of 15°. Based on the discussion in Section 2.2.1, we can see that this is because as the bending angle increases, the impact force on the outer-layer materials is reduced, which makes the distribution of the impact force on the threshing teeth more uniform and thus the proportion of broken grains is decreased. However, as the bending angle increases further, the impact force decreases slightly (Tan et al., 2023), and the ability of the threshing teeth to grasp the materials is reduced, resulting in a longer retention time of the materials in the threshing drum. As a result, the number of collisions between the materials and the threshing teeth is increased, and the proportion of broken grains is increased slightly.

The minimum and maximum proportions of broken grains with both traditional and arc-shaped threshing teeth are obtained for drum speeds of 500 r·min^{-1} and 600 r·min^{-1}, respectively. As shown in Figure 4, for a given drum speed, the 15° arc-shaped teeth produce the lowest proportion of broken grains (i.e. better than for traditional threshing teeth). When the drum speed is 500 r·min^{-1}, the minimum proportion of broken grains, with a value of 0.61%, is obtained for the 15° arc-shaped teeth. At this drum speed, the proportion of broken grains for the traditional threshing teeth is 1.29%, giving a difference of 0.68% between the two. This difference arises because although the traditional threshing teeth are bent at a certain angle, the straight sides of the teeth cause the striking force to be unevenly distributed along the entire length of each tooth. Moreover, the ability of the traditional teeth to grasp the threshed materials is significantly weakened by the large bending angle, resulting in a relatively high proportion of broken grains. In contrast, when 15° arc-shaped teeth are adopted, the impact force on the outer layer of materials is reduced, and the distribution of the impact force along the entire threshing tooth is relatively uniform; this avoids significant weakening of the ability to grasp the material, leading to a relatively low proportion of broken grains.

Due to the uneven distribution of the striking force of the traditional threshing teeth, the proportions of broken grains for 20° and 25° arc-shaped teeth are also lower than for traditional threshing teeth for the same rotational speed of the drum, but are slightly higher than for the 15° arc-shaped teeth. At a drum speed of 500 r·min^{-1}, the proportions of broken grains for the 20° and the 25° arc-shaped teeth are 0.72% and 0.79%, respectively, representing differences from the values for traditional threshing teeth of 0.57% and 0.5%, respectively. When the bending angles of the arc-shaped teeth are less than 15°, the proportion of broken grains remains higher than for traditional threshing teeth. This is because although the impact force on the outer layer of material decreases as the bending angle becomes smaller, this decrease is not significant, and the impact force is still unevenly distributed along the teeth. In addition, the bending reduces the ability to grasp the materials, leading to a higher proportion of broken grains.

The maximum proportion of broken grains (2.33%) is obtained for the 10° arc-shaped teeth and a drum speed of 600 r·min^{-1}, whereas the equivalent value for traditional threshing teeth is 1.87%, a difference of 0.46%. In summary, when 15° arc-shaped teeth are adopted, the proportion of broken grains can be significantly reduced, and the threshing quality can be effectively improved, thus demonstrating the excellent applicability and sufficient feasibility of this approach for practical operation.

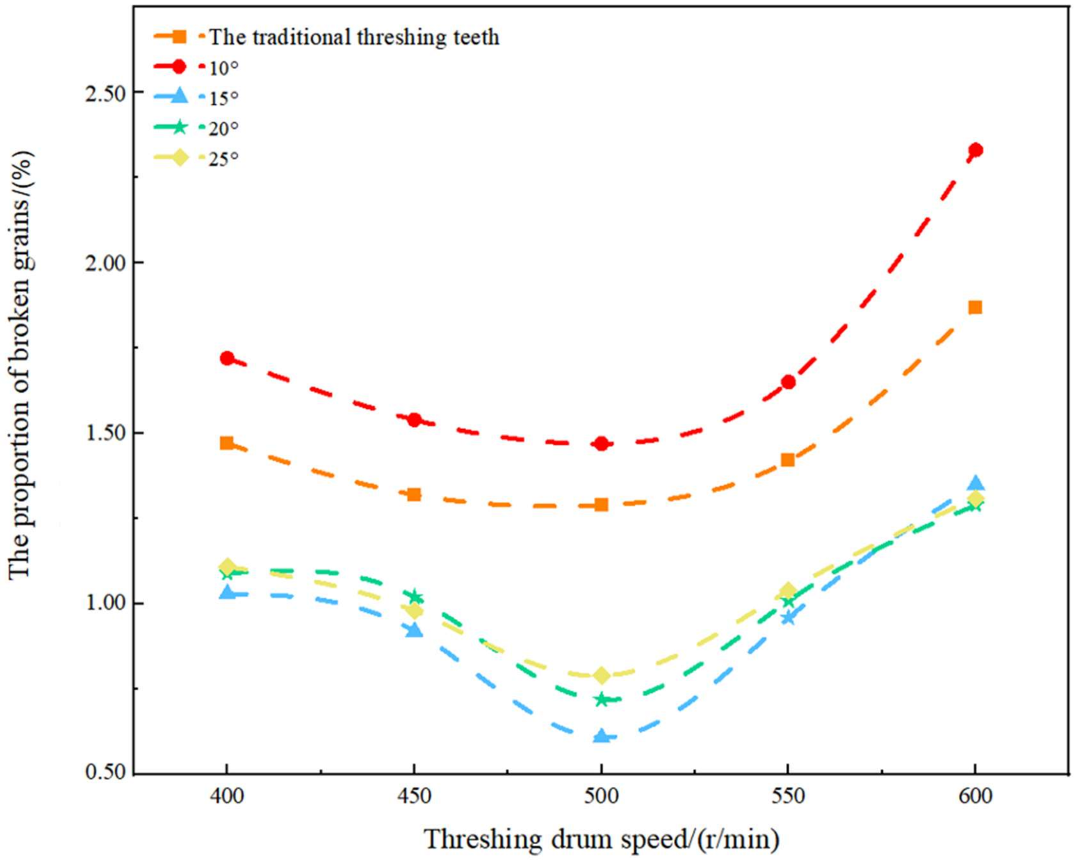

FIGURE 4. Influence of the drum speed on the proportion of broken grains.

Influence of drum speed on the proportion of unthreshed grains with different tooth shapes

Figure 5 shows the variation in the proportion of unthreshed grains with an increase in the drum speed, for different tooth shapes. As the drum speed increases, the proportion of unthreshed grains initially decreases and then increases. This is because the increase in the drum speed enhances the threshing intensity, which initially reduces the proportion of unthreshed grains; however, as the drum speed increases further, the transportation speed of the materials is increased, causing the soybean pods to be transported out of the drum before threshing and thus increasing the proportion of unthreshed grains (Kang et al., 2023).

The minimum proportions of unthreshed grains for both the traditional and the arc-shaped teeth are obtained at a drum speed of 500 r·min^{-1}, while the maximum proportions are obtained at a drum speed of 600 r·min^{-1}. As the bending angle of the threshing teeth increases, the proportion of unthreshed grains first increases and then slowly decreases, consistent with the discussion in Section 2.2.1. When the bending angle is increased, the impact force on the outer layer of material decreases, resulting in an increase in the proportion of unthreshed grains. However, when the bending angle is increased further, the impact force decreases to a small extent, and the ability of the threshing teeth to grasp the materials decreases. As a result, the residence time of the materials in the drum becomes longer, leading to an increase in the number of collisions between the materials and the threshing teeth, meaning that the proportion of unthreshed grains decreases slightly. At the same time, due to the increase in the number of collisions, the number of broken pods increases, which increases the difficulty of cleaning. For a given drum speed, the proportion of unthreshed grains is lowest when the bending angle is 10°. When the drum speed is 500 r·min^{-1}, the minimum proportion of unthreshed grains (1.42%) is obtained for the 10° arc-shaped teeth, while the minimum proportion for the traditional threshing teeth is 2.12%, representing a difference of 0.7%. This is because the bending angle of the 10° arc-shaped teeth is smaller than for the traditional threshing teeth, resulting in a greater impact force and a smaller proportion of unthreshed grains. The 15° arc-shaped teeth give the highest proportion of unthreshed grains under the same drum speed.

When the drum speed is 600 r·min^{-1}, the maximum proportion of unthreshed grains, with a value of 2.95% is achieved by the 15° arc-shaped teeth. At this drum speed, the proportion of unthreshed grains for the traditional teeth is 2.68%, representing a difference of 0.27%. This is because the 15° arc-shaped teeth make the impact force distribution more uniform while also reducing the impact force. Although the bending angle of the second segment of the traditional threshing teeth is greater than 15°, due to their straight structure, a relatively large impact force is generated. A larger angle also causes the grasping ability of the traditional threshing teeth to be reduced. As a result, the number of collisions between the materials and the threshing teeth is increased. Hence, at the same drum speed, the proportion of unthreshed grains for the traditional threshing teeth is lower than for the 15° arc-shaped teeth.

The proportion of unthreshed grains for the 20° arc-shaped teeth is slightly lower than for the 15° arc-shaped teeth and slightly higher than for the traditional threshing teeth under the same drum speed. When the drum speed is 500 r·min^{-1}, the proportion of unthreshed grains is 2.22%, representing a difference of 0.1% from the traditional threshing teeth at this drum speed. This is because the uneven distribution of the impact force of the traditional threshing teeth makes the impact force higher than for the 20° arc-shaped teeth, resulting in the proportion of unthreshed grains of the traditional threshing teeth being slightly lower than for the 20° arc-shaped teeth.

The proportion of unthreshed grains for the 25° arc-shaped teeth is slightly lower than for the traditional threshing teeth under the same drum speed. At a drum speed of 500 r·min^{-1}, the proportion of unthreshed grains is 2.07%, a difference of 0.05% from the traditional threshing teeth. This is because when the bending angle is 25°, the ability of the teeth to grasp the outer layer of materials is lower than for the traditional threshing teeth, and the increased number of collisions between the materials and the teeth leads to a slight decrease in the proportion of unthreshed grains. In summary, the optimal selection for the lowest proportion of unthreshed grains is the 10° arc-shaped teeth.

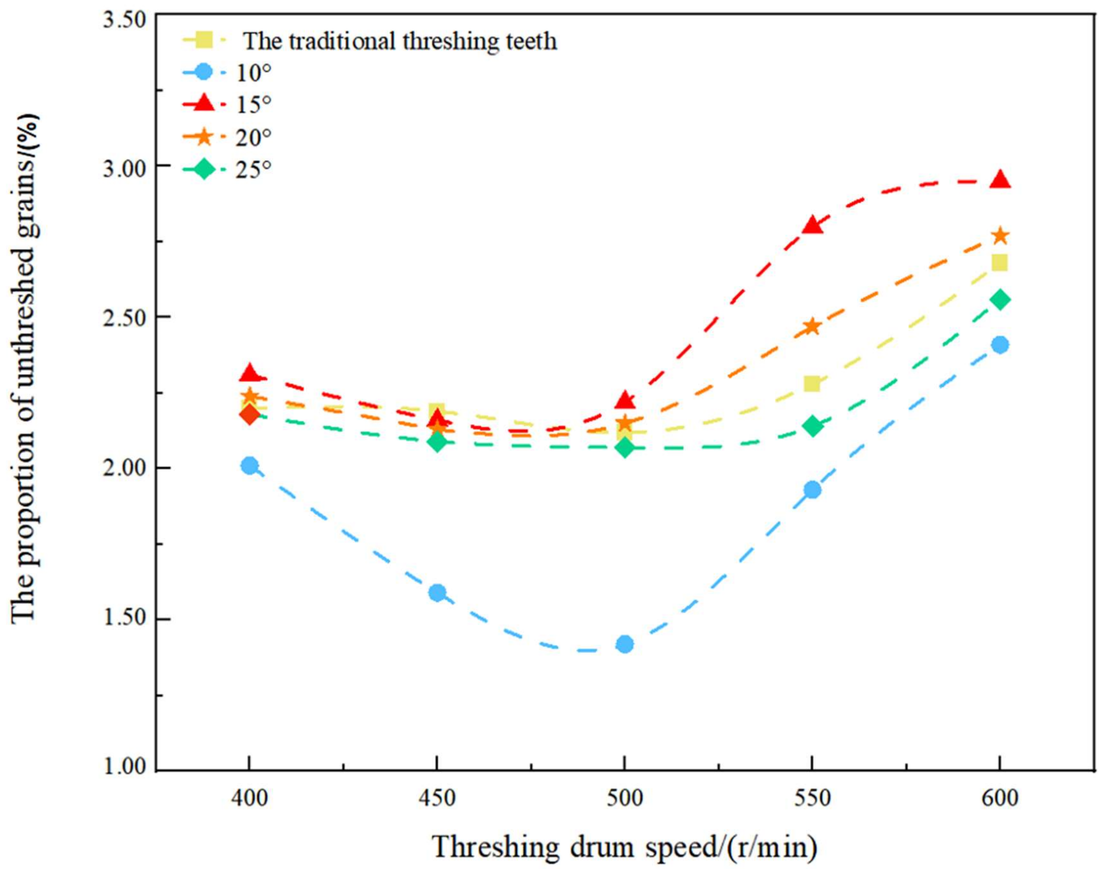

FIGURE 5. Influence of the drum speed on the proportion of unthreshed grains.

CONCLUSIONS

To address the issue of the high proportions of broken and unthreshed grains with traditional threshing teeth, the shape of the teeth was optimised. Four different arc-shaped teeth with varying bending angles were designed based on a logarithmic spiral. Bench tests were conducted to compare the threshing performance of these arc-shaped teeth to identify those with lower proportions of broken and unthreshed grains.

To achieve the lowest proportion of broken grains, the 15° arc-shaped teeth should be selected. At a drum speed of 500 r·min^{-1}, the proportion of broken grains is minimised to 0.61%, a value 0.68% lower than for traditional threshing teeth. Furthermore, this approach outperforms the arc-shaped teeth designed by Tan et al. (2023) under their optimal test conditions with regard to the proportion of broken grains, with a reduction of 0.143%. At this drum speed, the proportion of unthreshed grains is 2.22%, a value 0.1% higher than for the traditional threshing teeth.

To achieve the lowest proportion of unthreshed grains, the 10° arc-shaped teeth should be selected. At a drum speed of 500 r·min^{-1}, the proportion of unthreshed grains is minimised to 1.42%, a value 0.7% lower than for the traditional threshing teeth. At this drum speed, the proportion of broken grains is 1.47%, 0.18% higher than for the traditional threshing teeth.

To optimise the proportions of both broken and unthreshed grains, the 15° arc-shaped teeth should be selected, with a threshing drum speed of 500 r·min^{-1}. At this setting, the proportions of broken and unthreshed grains are at relatively low levels. According to GB/T 5982-2017, the acceptable proportions of broken and unthreshed grains for soybean threshers are ≤ 3% and ≤

5%, respectively. The proportions of broken (0.61%) and unthreshed grains (2.22%) under this combination meet the standard requirements.

This study has considerable significance. From a practical perspective, at the optimal drum speed of 500 r·min^{-1}, the 15° arc-shaped threshing teeth demonstrate excellent threshing performance, and can be directly applied to the upgrading and modification of the 5TD-1200 soybean thresher. This will help reduce losses during soybean harvesting and further improve the economic benefits of farmers. In theory, the design method established in this research for logarithmic spiral arc teeth can be extended to the optimisation of threshing components for other crops, such as corn and sunflowers, and provides a universal theoretical framework for low-damage design of threshing parts for agricultural machinery.

This research has the following limitations. Firstly, regarding the material used, only the "Heihe 43" soybean variety from Northeast China was considered in the experiments, and the impacts of different moisture contents and varieties on threshing performance were not accounted for. The universality of the conclusions therefore requires further verification. Secondly, in terms of the device parameters, the relationship between the concave plate clearance and the parameters of the arc-shaped tooth was not explored, meaning that opportunities for the joint optimisation of tooth type, clearance and drum speed may have been overlooked. These aspects will be considered and improved in future research.

ACKNOWLEDGEMENTS

This work was supported by the National Natural Science Foundation of China (Grant No. 52205253), the National Natural Science Foundation of Heilongjiang Province of China (Grant No.LH2022E007) and the Key Laboratory of High Efficient Seeding and Harvesting Equipments, Ministry of Agriculture and Rural Affairs of the People's Republic of China, Northeast Agricultural University, Harbin 150030, China (Grant No. 55200412).

DATA AVAILABILITY STATEMENT

The datasets generated during and analyzed during the current study are available from the corresponding author on reasonable request.

REFERENCES

Cabanos, C., Matsuoka, Y., & Maruyama, N. (2021). Soybean proteins/peptides: A review on their importance, biosynthesis, vacuolar sorting, and accumulation in seeds. *Peptides*, *143*. https://doi.org/10.1016/j.peptides.2021.170598

Chen, Z. P., Wassgren, C., & Ambrose, R. P. K. (2022). Development and validation of a DEM model for predicting impact damage of maize kernels. *Biosystems Engineering*, *224*, 16-33. https://doi.org/10.1016/j.biosystemseng.2022.09.012

Deng, J., Zhang, Q., Ma, X., Ren, F., Dong, Y. L., Yang, B. H., Zhu, H. C., Gong, X. D., Ouyang, Y. D., & Chen, B. H. (2018). *Testing methods for threshers*: *GB/T 5982-2017* [S]. Standards Press of China.

Dong, J. Q., Zhang, D. X., Yang, L., Cui, T., Zhang, K. L., He, X. T., Wang, Z. D., & Jing, M. S. (2023). Discrete element method optimisation of threshing components to reduce maize kernel damage at high moisture content. *Biosystems Engineering*, *223*, 221-240. https://doi.org/10.1016/ j.biosystemseng.2023.08.005

Fang, X. W., Zhang, J. S., Zhao, X. L., Zhang, L., Zhou, D. Y., Yu, C. S., Hu, W., & Zhang, Q. (2024). Optimising maize threshing by integrating DEM simulation and interpretive enhanced predictive modelling. *Biosystems Engineering*, *244*, 93-106. https://doi.org/10.1016/j.biosystemseng. 2024.06.001

Gao, L. X., Zheng, S. Y., Chen, R. X., & Yang, D. X. (2015). Design and experiment on soybean breeding thresher of double feeding roller and combined threshing cylinder. *Transactions of the Chinese Society for Agricultural Machinery*, *46*(1), 112-118. https://doi.org/10.6041/ j.issn.1000-1298.2015.01.017

Geremew, M., Molla, A., Gabbiye, N., Harvey, J., Mahroof, R., & Abay, F. (2023). Effects of threshing and storage conditions on post-harvest insect infestation and physical characteristics of maize grain. *Journal of Stored Products Research*, *103*. https://doi.org/10.1016/j.jspr.2023.102131

Hao, W. L., Liu, H. X., Zhu, L., Yang, Z. W., Cui, J. K., Liu, Z. J., Zhang, X. S., Xie, H., Zhao, J. Z., Li, M., Wang, Y. Y., Wang, F. Z., & Li, J. W. (2008). *General regulations for the determination methods of test conditions for agricultural machinery: GB/T 5262-2008* [S]. Standards Press of China.

Jia, H., Wang, Y. P., & Yang, J. (2025). Numerical investigation of coarse granular flow of the Coandă effect-based collector over logarithmic spiral surface for deepsea mining. *Applied Ocean Research*, *158*. https://doi.org/10.1016/j.apor.2025.104540

Jin, C. Q., Kang, Y., Guo, H. X., Wang, T. E., & Yin, X. (2021). Experimental research on the influence of threshing roller structures on the quality of mechanically-harvested soybeans. *Transactions of the Chinese Society of Agricultural Engineering*, *37*(4), 49-58. 10.11975/j.issn.1002-6819.2021.04.007

Kang, J. X., Wang, X. S., Xie, F. P., Luo, Y., Li, Q., & Huang, X. J. (2023). Experiments and analysis of the differential threshing cylinder for soybean with different maturities. *Transactions of the Chinese Society of Agricultural Engineering*, *39*(1), 38-49. https://doi.org/10.11975/j.issn.1002-6819.202206166

Lian, G. D., Wei, X. X., Ma, L. N., Zhou, G. H., & Zong, W. Y. (2022). Design and experiments of the axial-flow spiral drum threshing device for the edible sunflower. *Transactions of the Chinese Society of Agricultural Engineering*, *38*(17), 42-51. https://doi.org/10.11975/j.issn.1002-6819.2022.17.005

Liu, J. (2017). The design and experiment of low damage threshing mechanism of soybean harvester. Chinese Academy of Agricultural Sciences.

Liu, W. R., Zhou, Y., Xu, H. M., Fu, J. W., Zhang, N., Xie, G., & Zhang, G. Z. (2023). Optimization and experiments of the drum longitudinal axial threshing cylinder with rod tooth for rice. *Transactions of the Chinese Society of Agricultural Engineering*, *39*(15), 34 - 45. https://doi.org/10.11975/j.issn.1002-6819.202305076

Srison, W., Chuan-Udom, S., & Saengprachatanarak, K. (2016). Effects of operating factors for an axial-flow corn shelling unit on losses and power consumption. *Agriculture and Natural Resources*, *50*(5), 421-425. https://doi.org/10.1016/j.anres.2016.05.002

Su, Y., Liu, H., Xu, Y., Cui, T., Qu, Z., & Zhang, D. X. (2018). Optimization and experiment of spike-tooth elements of axial flow corn threshing device. *Transactions of the Chinese Society for Agricultural Machinery*, *40*, 258 - 265. https://doi.org/10.6041/j.issn.1000-1298.2018.S0.034

Tan, Y. F. (2023). Design and experiment of threshing device based on 4LZ-1.6Z soybean combine harvester. *Sichuan Agricultural University.* https://doi.org/10.27345/d.cnki.gsnyu. 2023.000290

Xing, S. L., Cui, T., Zhang, D. X., Yang, L., He, X. T., Li, C., Dong, J. Q., Jiang, Y. Y., Wu, W., Zhang, C. K., & Du, Z. H. (2024). Design and optimization for a longitudinal-flow corn ear threshing device of low loss and low energy consumption. *Computers and Electronics in Agriculture*, *226*. https://doi.org/10.1016/j.compag.2024.109328

Yang, X. Y., Li, B., Wang, S. G., Liu, Y., Dong, Y. C., & Liu, X. X. (2024). Design and trial of axial bow-tooth sunflower threshing device. *Agricultural Research in the Arid Areas*, *42*(3), 287-298. https://doi.org/10.7606/j.issn.1000-7601.2024.03.30

Zeng, Y., Huang, B., Qin, D., Zhou, S., & Li, M. (2022). Numerical and experiment investigation on novel guide vane structures of turbo air classifier. *Processes*, *10*(5), 844. https://doi.org/10.3390/pr1005084

Xie, F. P., Luo, X. W., Lu, X. Y., Sun, S. S., Ren, S. G., & Tang, C. Z. (2009). Threshing principle of flexible pole-teeth roller for paddy rice. *Transactions of the CSAE*, 25(8), 110 - 114. https://doi.org/10.3969/j.issn.1002-6819.2009.08.020